ACCOUNTS
of chemical research

Theoretical Aspects of the Biological Catch Bond

OLEG V. PREZHDO* AND YURIY V. PEREVERZEV
Department of Chemistry, University of Washington, Seattle, Washington 98195

RECEIVED ON SEPTEMBER 17, 2008

CONSPECTUS

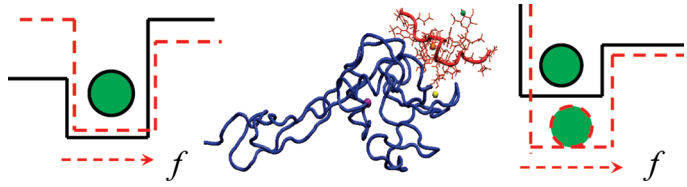

The biological catch bond is fascinating and counterintuitive. When an external force is applied to a catch bond, either *in vivo* or *in vitro*, the bond resists breaking and becomes stronger instead. In contrast, ordinary slip bonds, which represent the vast majority of biological and chemical bonds, dissociate faster when subjected to a force. Catch-bond behavior was first predicted theoretically 20 years ago and has recently been experimentally observed in a number of protein receptor−ligand complexes. In this Account, we review the simplest physical-chemical models that lead to analytic expressions for bond lifetime, the concise universal representations of experimental data, and the explicit requirements for catch binding.

The phenomenon has many manifestations: increased lifetime with growing constant force is its defining characteristic. If force increases with time, as in jump-ramp experiments, catch binding creates an additional maximum in the probability density of bond rupture force. The new maximum occurs at smaller forces than the slip-binding maximum, merging with the latter at a certain ramp rate in a process resembling a phase transition. If force is applied periodically, as in blood flows, catch-bond properties strongly depend on force frequency.

Catch binding results from a complex landscape of receptor−ligand interactions. Bond lifetime can increase if force (i) prevents dissociation through the native pathway and drives the system over a higher energy barrier or (ii) alters protein conformations in a way that strengthens receptor−ligand binding. The bond deformations can be associated with allostery; force-induced conformational changes at one end of the protein propagate to the binding site at the other end.

Surrounding water creates further exciting effects. Protein−water tension provides an additional barrier that can be responsible for significant drops in bond lifetimes observed at low forces relative to zero force. This strong dependence of bond properties on weak protein−water interactions may provide universal activation mechanisms in many biological systems and create new types of catch binding. Molecular dynamics simulations provide atomistic insights: the molecular view of bond dissociation gives a foundation for theoretical models and differentiates between alternative interpretations of experimental data.

The number of known catch bonds is growing; analogs are found in enzyme catalysis, peptide translocation through nanopores, DNA unwinding, photoinduced dissociation of chemical bonds, and negative thermal expansion of bulk materials, for example. Finer force resolution will likely provide many more. Understanding the properties of catch bonds offers insight into the behavior of biological systems subjected to external perturbations in general.

Introduction: Catch-Bond Prediction and Discovery

Binding of biological macromolecules through weak, noncovalent interactions is critical for living organisms. Catch binding represents one of many fascinating and counterintuitive phenomena that arise in complex biological systems. As often happens in science, the basic theory was suggested first, and experimental proof came much later. Dembo et al.[1] introduced the concept with mathematical description of membrane-surface adhesion. Catch bond was defined as a bond whose lifetime increased when it was stretched by a mechanical force. In contrast, life-

Published on the Web 03/30/2009 www.pubs.acs.org
10.1021/ar800202z CCC: $71.50

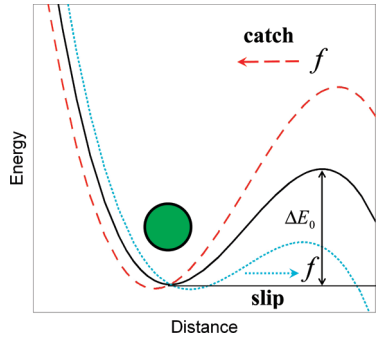

FIGURE 1. Effect of applied force on receptor−ligand interaction potential with barrier ΔE_0. Solid line shows force-free potential. In slip binding, force lowers the barrier (···) and favors bond dissociation. Catch binding occurs when force directed from the barrier toward the minimum raises the barrier (−−−).

times of ordinary slip bonds decrease during stretching. It was generally assumed that biological receptor−ligand complexes are slip bonds.[2] However, catch bonds were demonstrated recently. In 2002, flow-chamber experiments[3] reported force-enhanced cell adhesion, which could be rationalized by catch binding between lectin-like bacterial adhesion protein FimH and mannose ligands.[4] The first definitive demonstration[5] came in 2003 with atomic force microscope (AFM) studies of the P-selectin protein, expressed on endothelial cells and platelets, interacting with the PSGL-1 ligand expressed on leukocytes. The AFM experiments showed that beyond a critical force value, catch bonds behaved as ordinary slip bonds. The bond lifetime first increased but ultimately decreased with growing force.[5,6] The growth and subsequent decrease of the binding strength was also observed in flow-chamber experiments on FimH-mediated attachment of bacteria to host cells[3] and beads to surfaces.[7] More recently, catch−slip behavior was established in the actin/myosin complex.[8]

One expects that catch bonds evolved in response to the biological conditions in which they function. For instance, bonds involving selectins operate in blood flows.[9,10] Catch binding may prevent spontaneous aggregation of flowing leukocytes in capillaries and postcapillary venules, where forces on the bonds are low.[11]

Catch and Slip Bonds

To understand the intermolecular forces involved in catch binding, consider the energy of receptor−ligand interaction, Figure 1. The larger is the height ΔE_0 of the barrier separating the bound state from the dissociated state, the longer is the bond lifetime. According to Bell,[2] applied forces f induce linear changes in barrier height

$$\Delta E(f) = \Delta E_0 \pm \Delta x f \quad (1)$$

where Δx is barrier width. The sign in front of Δx reflects force direction. It is negative, if force pulls the ligand out. This situation was considered originally by Bell.[2] The sign is positive, if force pushes the ligand in. This possibility was first discussed by Dembo et al.[1] The former situation describes slip bonds, since force promotes bond breaking. If the free-energy landscape of receptor−ligand interaction is such that force pushes the ligand deeper into the receptor, the complex behaves as a catch bond. Ultimately, all known catch bonds transition to slip bonds given sufficient force.

A number of explanations of the catch−slip transition have been proposed.[12−17] A simple description is provided by the two-pathway model,[15] which offers both catch and slip pathways for bond dissociation, Figure 2a. The catch pathway involves a low energy barrier. By increasing the catch barrier and decreasing the slip barrier, force compels the bond to switch from the catch to the slip pathway. Bond lifetime is maximized when force equalizes the barrier heights. Important experimental facts can be explained with a potential containing two bound states and two dissociation pathways,[13,14,17] Figure 2b.

The bond-deformation model[16] provides an alternative to the two-pathway idea. It argues that force lowers the potential energy minimum by changing bond structure, Figure 2c. Essential for catch binding, the minimum should drop faster than the top of the barrier, which evolves by the Bell mechanism as before. In contrast to the two-pathway model, the deformation model needs just one dissociation pathway. An allosteric form of catch-bond deformation has been suggested by experiment and atomistic simulation.[11,18−21] Large-scale conformational changes correlate with increased bond lifetimes, Figure 2d, and are stabilized by either applied force or interaction with another ligand.[18]

Catch binding has been attributed to higher-order fluctuation effects[22] that extend beyond the Bell mechanism. Further complications are provided by the force-history dependence of bond rupture.[23]

Atomistic simulations suggest that in order to escape, the ligand must overcome a number of barriers and bound states, giving rise to the sliding−rebinding mechanism,[24,25] Figure 2e.

Two-Pathway Model

The receptor−ligand interaction potential contains a single bound state, x_1, and two barriers, x_c and x_s, leading to the unbound state 0, Figure 3a. Force raises the catch barrier and lowers the slip barrier. The two-pathway model,

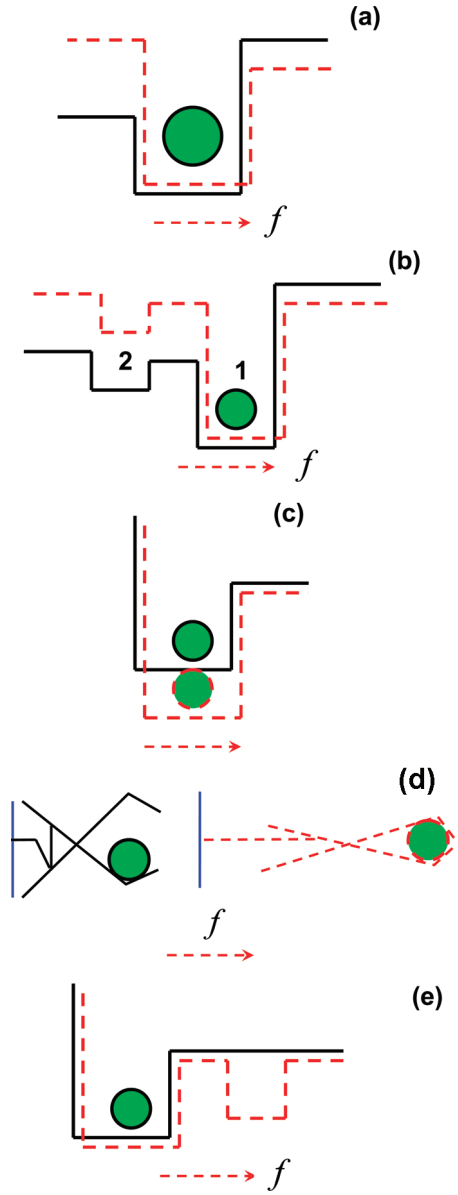

FIGURE 2. Catch-bond models. Ligand (green circle) moves in the potential created by receptor−ligand interaction. Force transforms the potential, solid line into dashes. (a) Two-pathway model[15] includes single bound state and two barriers to bond dissociation. (b) Two-state, two-pathway model[13,14,17] contains two bound states and two dissociation barriers. (c) Deformation model[16] rationalizes catch binding as bound state lowering by force-induced deformation. (d) Allosteric deformation model[48] associates force-induced deformation that lowers the minimum, part c, with large-scale conformational changes initiated by allosteric interaction far from ligand. (e) Sliding−rebinding model[24] suggests that catch binding arises due to additional binding minima, which appear as ligand slides along receptor.

proposed conceptually in ref 6 and analyzed mathematically in refs 15, 26, and 27, captures essential features of the catch−slip transition. The model's simplicity yields many analytic results.

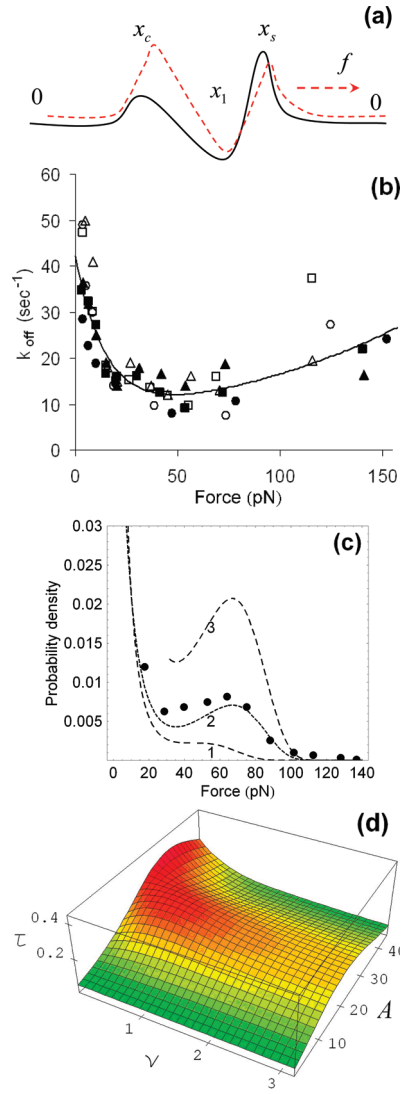

FIGURE 3. Two-pathway model.[15] (a) Ligand in bound-state x_1 escapes to free-state 0 over either slip, x_s, or catch, x_c, barrier. Initially (solid line), dissociation occurs primarily via the lower catch barrier. Force increases the catch barrier and decreases the slip barrier (dashes). Bond lifetime grows until the slip barrier drops below the catch barrier. (b) Constant force. Dissociation rate constant vs force for sPSGL-1 (unfilled symbols) and PSGL-1 (filled symbols) bound to L-selectin. Theoretical line agrees with experiment.[6] (c) Jump−ramp. Rupture force probability density for P-selectin/sPSGL-1. Points (●) show experimental data[13] for ramp rate, $r = 210$ pN/s, and jump force, $f_0 = 0$. Theoretical lines correspond to (1) critical ramp rate $r = r_c = 95.6$ pN/s characterizing onset of new maximum and $f_0 = 0$, (2) $r = 210$ pN/s and $f_0 = 0$ as in experiment, and (3) $r = 210$ pN/s and $f_0 = 30$ pN illustrating finite jump force. (d) Periodic force.[28] Lifetime τ (s) of P-selectin/PSGL-1 bond vs force frequency ν (s^{-1}) and amplitude α (pN), eq 14. Lifetime changes when frequency drops below 30 beats per minute (0.5 s^{-1}).

Constant Force Scenario. Bond survival probability for constant force is given by

$$P(t) = \exp(-t/\tau(f)) \qquad (2)$$

where inverse bond lifetime τ contains slip and catch contributions

$$1/\tau(f) = k_{1s}^0 \exp(x_{1s}f/(k_BT)) + k_{1c}^0 \exp(-x_{1c}f/(k_BT)) \quad (3)$$

The two-pathway model has four parameters: force-free dissociation rate constants for each pathway, k_{1c}^0 and k_{1s}^0, and barrier widths $x_{1c} = |x_c - x_1|$ and $x_{1s} = |x_s - x_1|$, defined by distances from the minimum, x_1, to the maxima, x_c and x_s, of the free-energy profile, Figure 3a. Catch binding occurs if

$$a = \frac{k_{1c}^0 x_{1c}}{k_{1s}^0 x_{1s}} > 1 \quad (4)$$

and lifetime is maximized at critical force

$$f_{cr} = \frac{k_BT}{x_{1s} + x_{1c}} \ln a \quad (5)$$

If $a \leq 1$, the bond always remains a slip bond.

Condition 4 requires the catch barrier to be lower and broader than the slip barrier. Indeed, force should pull the ligand over a less favorable pathway in order to increase bond lifetime. Therefore, the slip barrier must be higher than the catch barrier. Further, the catch barrier should increase faster than the slip barrier decreases and, therefore, should be broader, since the barrier height changes in proportion to its width, eq 1.

Catch binding can be quantified by the ratio of maximized bond lifetime to lifetime at zero force

$$\frac{\tau(f_{cr})}{\tau(0)} = \frac{x_{1s}(k_{1s}^0 + k_{1c}^0)}{k_{1c}^0(x_{1s} + x_{1c})} a^{x_{1c}/(x_{1s}+x_{1c})} \quad (6)$$

Equation 6 indicates that catch binding is efficient only when $k_{1c}^0 \gg k_{1s}^0$, that is, if the catch barrier is significantly lower than the slip barrier. Since barrier widths cannot vary as much as rate constants, which depend exponentially on barrier heights, the widths do not change the efficiency ratio (eq 6) significantly. Nevertheless, it is important that the catch barrier is wider than the slip barrier. Even if $k_{1c}^0 \gg k_{1s}^0$ and $a > 1$, the ratio (eq 6) approaches unity for $x_{1c} \ll x_{1s}$.

Figure 3b shows that the two-pathway model works very well. The efficiency ratio, eq 6, for sPSGL-1 and PSGL-1 bound to L-selectin[6] is small, around 4, because the rates for the two pathways differ little, $k_{1c}^0/k_{1s}^0 = 5$. The optimal force is relatively large, $f_{cr} = 50$ pN. The same ligands bound to P-selectin show a significantly higher catch binding efficiency, $\tau(f_{cr})/\tau(0) = 90$, at a smaller force, $f_{cr} = 10$ pN. The efficiency is higher, since $k_{1c}^0/k_{1s}^0 = 500$; f_{cr} is smaller because the barriers are wider.[15]

Both monomeric and dimeric bonds are possible in the PSGL-1/P-selectin system. Detailed analysis[15] of experiments[5] shows that if bond extension is kept constant and if the cantilever is stiffer than the proteins, then the force applied by the cantilever to the dimer is twice larger than the force acting on the monomer. As a result, the dimer and monomer lifetimes are related by a simple relationship, $\tau_{dimer}(f) = {}^3/_2\tau_{monomer}(f/2)$, that correctly describes[15] the experimental data.[5]

Jump−Ramp Scenario. In the jump−ramp scenario,[13] the force jumps to f_0 and then gradually grows with ramp rate r

$$f(t) = f_0 + rt \quad (7)$$

Experimental data are presented with rupture force histograms[13] corresponding to probability density[26]

$$p(f,f_0) = \frac{1}{r\tau(f)} \exp\left[-\frac{k_BT}{r} g(f,f_0)\right] \quad (8)$$

where $\tau(f)$ is bond lifetime for constant force, eq 3,

$$g(f,f_0) = \varphi(f) - \varphi(f_0), \quad \varphi(f) = \frac{k_{1s}^0}{x_{1s}} \exp\left(\frac{x_{1s}f}{k_BT}\right) - \frac{k_{1c}^0}{x_{1c}} \exp\left(\frac{-x_{1c}f}{k_BT}\right) \quad (9)$$

and $f \geq f_0$.

The shape of probability density (eq 8) depends on the critical ramp rate, r_{cr}. If $r < r_{cr}$, it monotonically decreases with force for both catch and slip bonds. If $r > r_{cr}$, it develops a characteristic catch minimum, Figure 3c. One can show that the locations of the minimum and maximum are independent on f_0 but the magnitude of the maximum shows double-exponential dependence on f_0.

Generally, for jump−ramp experiments, catch bonds can be distinguished from slip bonds by the minimum in the rupture force probability density, as well as by increased probability of bond dissociation at low forces. Detecting the minimum requires sufficiently high ramp rates. Both catch-bond features are masked by large jump forces. Therefore, one should use large ramp rates and small jump forces.

Universal Laws. Universal laws[27] establish profound relationships between experiments carried out under different conditions and allow one to detect and investigate discrepancies that can lead to better experiments and, ultimately, new discoveries.

For example, eq 8 relates jump−ramp probability density to constant force lifetime, which can be immediately extracted from jump−ramp data, $\tau(f_0) = 1/(rp(f_0,f_0))$. Exponential dependence of rate constants, eq 3, gives universal laws that eliminate some experimental parameters.[27] Combining probability

densities for different ramp rates, r and r', and the same jump force, f_0, removes ramp rate:

$$\frac{rr'}{k_BT(r - r')} \ln\left[\frac{rp(f, r; f_0)}{r'p(f, r'; f_0)}\right] = g(f, f_0) \quad (10)$$

Both ramp rate and force are eliminated by combining probabilities for different ramp rates and jump forces

$$\frac{1}{k_BT}[r \ln P(f, r; f_0) - r' \ln P(f, r'; f_0')] = g(f_0, f_0') \quad (11)$$

These equations place model-independent experimental observables on the left side and physical characteristics that follow from a specific model on the right side, testing different models against common experimental quantities.[27]

Periodic Perturbation. Catch bonds operating in blood flows are subject to oscillatory perturbations. Reference 28 makes an intriguing prediction showing that properties of the PSGL-1/P-selectin bond change dramatically at a critical frequency.

Figure 3d shows bond lifetime vs force frequency, $\nu = \omega/(2\pi)$, and amplitude, A

$$f(t) = f_0 + A \sin(\omega t) \quad (12)$$

Background force f_0 describes the average effect of blood flow.[29] In Figure 3d, $f_0 = A$. For a stationary regime, the bond is most stable when $A = 32.3$ pN. Oscillation reduces the optimal force to $A = 21.5$ pN.

Bond properties change at physiologically relevant frequencies of 0−30 beats per minute and are not sensitive to further frequency increase. For comparison, the slowest human heart rates known with endurance athletes at rest reside around 30 beats per minute. Slower rates are considered pathological. Catch bonds may have evolved to preserve their properties for normal heart rates. Investigating catch bonds of nonhuman selectins, for instance, those of rodents with their much higher heart rates, can provide further tests of this hypothesis.

Deformation Model

Protein structure can notably change during bond formation. Similar effects are expected when proteins are subjected to mechanical forces. Residues that come in contact inside the binding pocket can shift, thereby improving or weakening receptor−ligand interactions. Bond deformation can act in addition to the Bell renormalization of barrier height.

Figure 4a illustrates the bond deformation effect. The force optimizes the distance between ligand atoms x_1 and x_2 to match receptor size b. Analysis shows that receptor−ligand interaction energy is linear in f for small f. Changes should saturate at a certain force f_0, for instance, if the bond resists further deformation or deformation continues outside the binding pocket. These two considerations motivate the functional form of deformation energy

$$\Delta E_d(f) = \alpha[1 - \exp(-f/f_0)] \quad (13)$$

Combined with the Bell term, eq 13 gives the following rate constant

$$k(f) = k_0 \exp\left[-\frac{\Delta E_d(f) - x_{12}f}{k_BT}\right] \quad (14)$$

Similarly to the two-pathway model, the deformation model contains four parameters: force-free rate constant k_0, barrier width x_{12}, deformation energy α, and saturation force f_0. It provides comparable fits of the experimental data, Figure 4b,c. In contrast to the two-pathway model, the deformation describes the catch−slip transition using only one dissociation pathway.

Bond lifetime is maximized by the critical force

$$f_{cr} = f_0 \ln[\alpha/(x_{12}f_0] \quad (15)$$

and catch binding efficiency is

$$\frac{\tau(f_{cr})}{\tau(0)} = \exp\left[\frac{\alpha - x_{12}(f_0 + f_{cr})}{k_BT}\right] \quad (16)$$

compared with eqs 5 and 6 for the two-pathway model. The efficiency can significantly exceed one if deformation energy is greater than the Bell term, $\alpha > x_{12}(f_0 + f_{cr})$.

Force-induced bond deformation is a general concept that can explain other phenomena. In particular, it rationalizes the disparity between bond dissociation rates measured in force-free experiments with those extrapolated from finite-force data to zero force.[16] The deviations between the asymptotic $k_{as} = k_0 \exp[-\alpha/(k_BT)]$ and true k_0 zero-force rate constants are determined by the bond deformation energy, which may be extracted directly from experiments:

$$\alpha = k_BT \ln(k_0/k_{as}) \quad (17)$$

Since α can be positive or negative, the asymptotic rate can be much greater or much less than the true rate. Large α imply that bonds are greatly affected by force. Small α indicate stiff bonds that resist perturbations. Most biological bonds have negative α, meaning that receptor−ligand interactions are optimized and diminish with bond deformation. Positive α indicate that deformation improves receptor−ligand binding. Catch binding requires $\alpha > x_{12}f_0$.

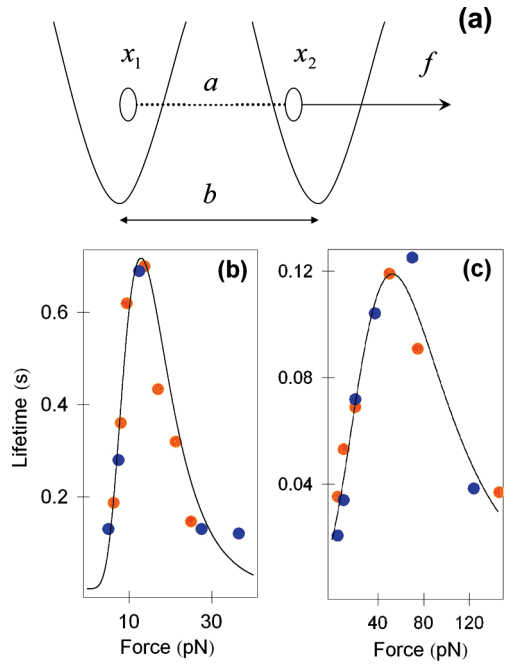

FIGURE 4. Deformation model.[16] (a) Force adjusts ligand atoms x_1 and x_2 relative to receptor potential, improving interaction. Lifetimes of (b) P- and (c) L-selectin bonds with monomeric sPSGL-1 (blue circles) and dimeric PSGL-1 (orange circles) vs force.[5,6,15] Model fits data well (solid line).

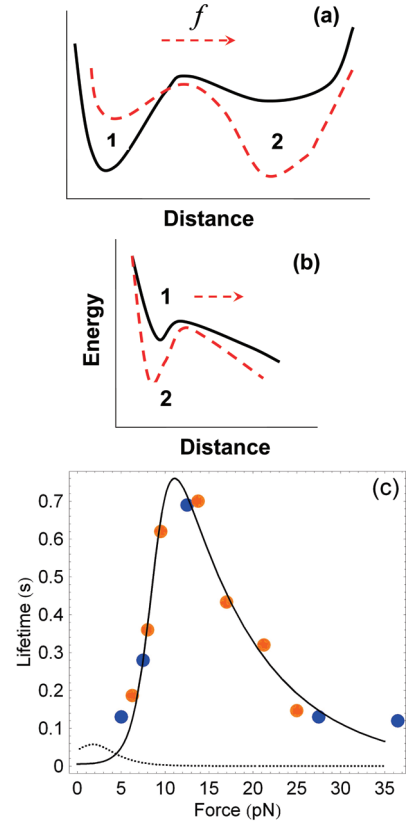

FIGURE 5. Allosteric deformation model.[48] (a) Potential responsible for large-scale conformational changes, Figure 2d. States "1" and "2" describe native and stretched conformations. (b) Receptor−ligand interaction potential deepens as receptor is stretched. (c) Experimental lifetimes (circles) of the P-selectin/PSGL-1 bond. Bond lifetime (solid line) is significantly longer than conformational relaxation time (dashes).

Allosteric Deformation Model

The deformation model discussed above focused on geometry changes near the binding site. Experiments and simulations show that catch binding is coupled to large-scale conformational rearrangements of receptor far from the binding site,[17,24,30−33] Figure 2d, suggesting allosteric interaction.[34,35] The allosteric site produces mechanical stresses that propagate through globular protein structure and deform the binding site.

Figure 5a shows potential describing native and stretched conformations of receptor, Figure 2d. Native state "1" is more stable initially. Force tilts the potential and makes stretched state "2" lower than "1". Solid and dashed lines illustrate the limits $f = 0$ and $f \gg 0$. As force grows, potential changes continuously between these limits. The probabilities for closed and open states, $P_1(t,f)$ and $P_2(t,f)$, are determined by the rate constant ratio $k_{12}(f)/k_{21}(f)$ describing transitions between "1" and "2". The force dependence is exponential, as in eq 3.

Receptor−ligand binding potential deepens, Figure 5b, when receptor is stretched. Bond dissociation rate constant for native state $k_1(f)$ is larger than for stretched state $k_2(f)$. The receptor conformation fluctuates, and the average rate constant is

$$k_r(t,f) = k_1(f)P_1(t,f) + k_2(f)P_2(t,f) \qquad (18)$$

If conformational fluctuation occurs faster than bond dissociation, bond deformation time $\tau_d(f)$ is shorter than catch-bond lifetime $\tau_c(f)$. The P-selectin/PSGL-1 data support this assumption, Figure 5c, leading to

$$\frac{1}{\tau_c(f)} = k_1^0\left[K + \frac{1-K}{1 + R\exp(2x_d f/(k_B T))}\right]\exp(x_b f/(k_B T)) \qquad (19)$$

The bond lifetime in the allosteric deformation model contains five parameters: widths of barriers between native and stretched states, x_d, Figure 5a, and between bound and free states, x_r, Figure 5b; and force-free rate-constants and their ratios $k_1(0)$, $K = k_2(0)/k_1(0)$ and $R = k_{12}(0)/k_{21}(0)$.

Allosteric deformation may explain catch binding in the mannose/FimH bond,[17] whose strength depends on conformations of lectin and pilin domains of FimH,[30−32,36,37] Figure 2d. The bond is weak when the domains are closed. It

strengthens when domains open up. Similar domain opening is revealed in P-selectin/PSGL-1 by atomistic simulation.[24,33]

Allosteric deformation couples protein conformation to receptor−ligand interaction. Allosteric effect acts both ways. Conformational rearrangements strengthen the interaction. Conversely, ligand binding induces conformational change.

Protein−Water Interaction

The protein−water interface can dramatically affect the response of biological bonds to small forces. Recently, several bonds showed large differences between bond lifetimes measured at zero and finite forces,[5,6,38−40] as demonstrated by the actin/myosin bond.[8] The measurement performed at $f = 0.07$ pN gave a 2.7 s lifetime. In comparison, the lifetime at $f = 1.5$ pN was 1.5×10^{-2} s, 2 orders of magnitude lower. Catch binding was observed between 1.5 and 5 pN, with the lifetime increasing to 3×10^{-2} s. For $f > 5$ pN, the lifetime decreased again. This catch−slip transition around $f \approx 5$ pN was well described by the deformation model.[41] The 100-fold lifetime drop somewhere between 0.07 and 1.5 pN required further rationalization.

Similar changes were observed with other catch and slip bonds. Surface plasmon resonance (SPR) revealed fast and slow ruptures of P-selectin/PSGL-1 bonds at low forces.[38,42] The lifetimes differed by 3 orders of magnitude: from 3.3×10^3 to 3 s. Further, AFM demonstrated lifetimes of 0.5 s or less at the lowest forces measured.[5,6] The streptavidin/biotin lifetime measured by AFM[39] was 100 s, while the SPR lifetime[40] equaled to 2.5×10^5 s.

These huge lifetime differences seen at zero and finite forces for a variety of biological bonds can occur due to protein−water interfacial tension, Figure 6a.[41] The interface is minimized when receptor and ligand are tightly bound. As ligand leaves the binding pocket, the interface increases and creates tension that opposes bond dissociation. The receptor−ligand interaction in aqueous environment can be described by a potential with two minima, Figure 6b. The deep minimum describes the intrinsic receptor−ligand interaction. Once ligand leaves the deep minimum, it encounters a shallow minimum followed by a wide barrier, which arise from protein−water surface tension.

The small depth and large width of the protein−water potential guarantee that it is suppressed by weak forces, dashes in Figure 6b. The critical force, f_c, eliminating the additional barrier defines two regimes: (A) $0 < f \leq f_c$, where both states "1" and "2" are present and (B) $f > f_c$, without state "2". Transition from A to B generates gigantic differences in bond lifetimes. The lifetime in case A is given by

$$\tau_A(f) = \frac{k_{21}(f)}{k_{2f}(f)k_{12}(f)}, \quad 0 < f < f_c \tag{20}$$

where $k_{12}(f)$ and $k_{21}(f)$ are rate constants for transitions from "1" to "2" and back, and $k_{2f}(f)$ describes transition from "2" to

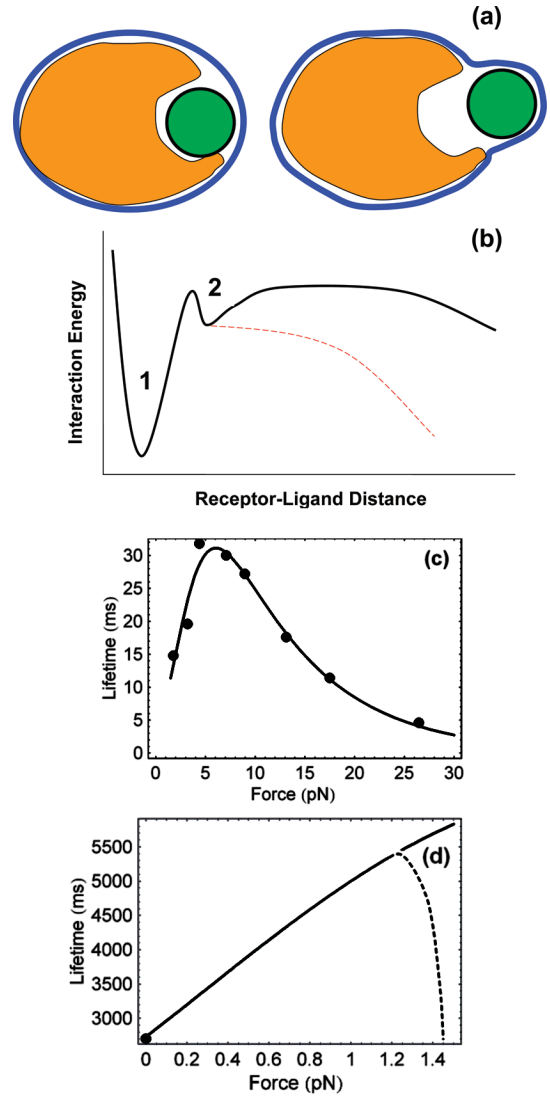

FIGURE 6. Effect of protein−water interaction on receptor−ligand binding. (a) Receptor and ligand surrounded by water: orange, green circle, and blue strip, respectively. Left, equilibrium conformation with water network optimized around the complex; right, protein−water interface grows; created surface tension opposes bond dissociation. (b) Receptor−ligand potential in water. Deep minimum "1" is formed by intrinsic receptor−ligand interaction. Shallow minimum "2" and broad barrier arise due to protein−water surface tension (solid line). Weak force suppresses protein−water barrier (dashes), leaving intrinsic interaction unaffected. (c) Lifetime of actin/myosin complex for $f \geq 1.5$ pN. Deformation model[16] fits experimental data (circles).[8] (d) Bond lifetime for $f < 1.5$ pN. Note different scales in panels c and d. Theory predicts new form of catch binding at low forces. When protein−water barrier disappears, bond lifetime precipitates (dashes).

free state. The bond lifetime in case B is

$$\tau_B(f) = 1/k_{12}(f), \quad f \geq f_c \tag{21}$$

where $k_{12}(f)$ is the same as $k(f)$ in eq 14.

Equation 20 makes two assumptions: $k_{21}(f) \gg k_{12}(f)$, since "2" is significantly more shallow than "1"; and $k_{21}(f) \gg k_{2f}(f)$, since the second barrier is much wider than the first. Both $k_{21}(f)$ and $k_{2f}(f)$ are essentially independent of force for $0 < f < f_c$. Therefore, eq 20 becomes $\tau_A(f) \approx (k_{21}(0))/(k_{2f}(0)k_{12}(f))$. Together with eq 21, this gives the following conclusions. First, the ratio of bond lifetimes between regimes A and B in the $f \rightarrow f_c$ limit is much greater than one, since $\tau_A(f_c)/\tau_B(f_c) \approx k_{21}(0)/k_{2f}(0) \gg 1$. Second, catch or slip binding type depends on intrinsic receptor−ligand interactions, $k_{12}(f)$, and is independent of protein−water tension.

The actin/myosin bond is long-lived at weak forces, Figure 6d. Once force suppresses the protein−water barrier, the lifetime dramatically drops, Figure 6c. The bond is now governed by intrinsic receptor−ligand interactions. Catch binding lasts as long as bond deformation continues to deepen the main minimum. When deformation saturates, the actin/myosin complex becomes a slip bond. Fascinatingly, low forces show a new catch binding type that is a combination of bond deformation and protein−water tension, Figure 6d.

Substantial changes in bond lifetime at small forces are independent of catch or slip bond type. Commonality of protein−water interactions suggests that the anomaly occurs in majority of biological receptor−ligand bonds.

An intriguing prediction can be made. The protein−water barrier keeps biological bonds in a latent state, which is activated by weak mechanical contacts, concentration gradients, and electric signals.[43−45]

Atomistic Simulation

Atomistic description of bond dissociation is useful for visualizing structural changes, interpreting experimental data, and discriminating between models. Steered molecular dynamics (SMD) investigates system response to external forces.[46]

Figure 7a,b compares typical SMD and experimental results. The two-pathway and deformation models with parameters fitted to experimental data are used to predict simulation data. Focusing on the jump−ramp protocol, eq 7, Figure 7a shows P-selectin/PSGL-1 dissociation probability density for zero jump force and experimental ramp rate $r = 500$ pN/s. The two maxima give catch and slip dissociations, similar to Figure 3c, but noting different abscissa units. The minimum characterizes the catch−slip transition; 40% of dissociations occur by the catch mechanism.

Figure 7b shows bond dissociation probability density for a much larger ramp rate, $r = 0.695 \times 10^{12}$ pN/s, typical of simulations that require strong forces. The increased ramp rate carries three major impacts. First, dissociation is significantly faster; compare time scales in Figure 7a,b. Second, the maximum becomes narrower and higher; compare probability density scales. Third, probability density is almost entirely shifted to the slip region; 98% of dissociations occur by the slip mechanism. Two practical conclusions can be made. Simulation is unlikely to produce catch examples. At the same time, slip behavior can be characterized by few trajectories, since the slip maximum is very narrow.

The crystal structure[47] indicates that PSGL-1 interacts with P-selectin in two locations, Figure 7c. The ligand's Tys-607 (Tys = sulfotyrosine) residue is attracted to receptor's loop containing Ser-46. At the other side of the binding pocket, the ligand's Fuc-623 (Fuc = fucose) is attracted to the calcium ion that binds to the receptor. The two interaction regions were probed by two sets of simulations, differing in the direction of the applied force.[33] One simulation probed the interaction mediated by the Ca^{2+} ion by pulling the ligand's end (END). The other simulation probed the Tys-607/Ser-46 interaction by pulling ligand's center of mass (COM).

The END simulation mimicked experiments and showed that the stronger bound Ca^{2+} site dissociated before the weaker Tys-607/Ser-46 interaction, even though the force required to break the Ca^{2+} interaction was twice that required to break the Tys-607/Ser-46 interaction, as determined by the COM simulation, Figure 7d. Since the stronger site ruptured first, it was responsible for the experimental observations.[5,13] The scenario in which the data were dominated by partial bond rupture at the weaker site was eliminated.

Simulations show large changes in the orientation of the EGF and lectin domains, Figure 7e. This is consistent with the allosteric deformation model, Figure 2d, and supports the sliding−rebinding mechanism, Figure 2e, in which domain opening aligns the binding site with the pulling direction.[24]

Experiment and simulation differ by many orders of magnitude and can be related only through models. Using experimental parameters, the two-pathway and deformation models predict 490 and 470 pN rupture forces for simulation. This is in good agreement with 460 pN obtained in simulations. It is remarkable that experiment, theory, and simulation agree over 9 orders of magnitude!

Currently, the two-pathway model[15,26−28] remains the most commonly used mathematical description of catch bonds; however, it may not reflect correct physics, particularly in systems

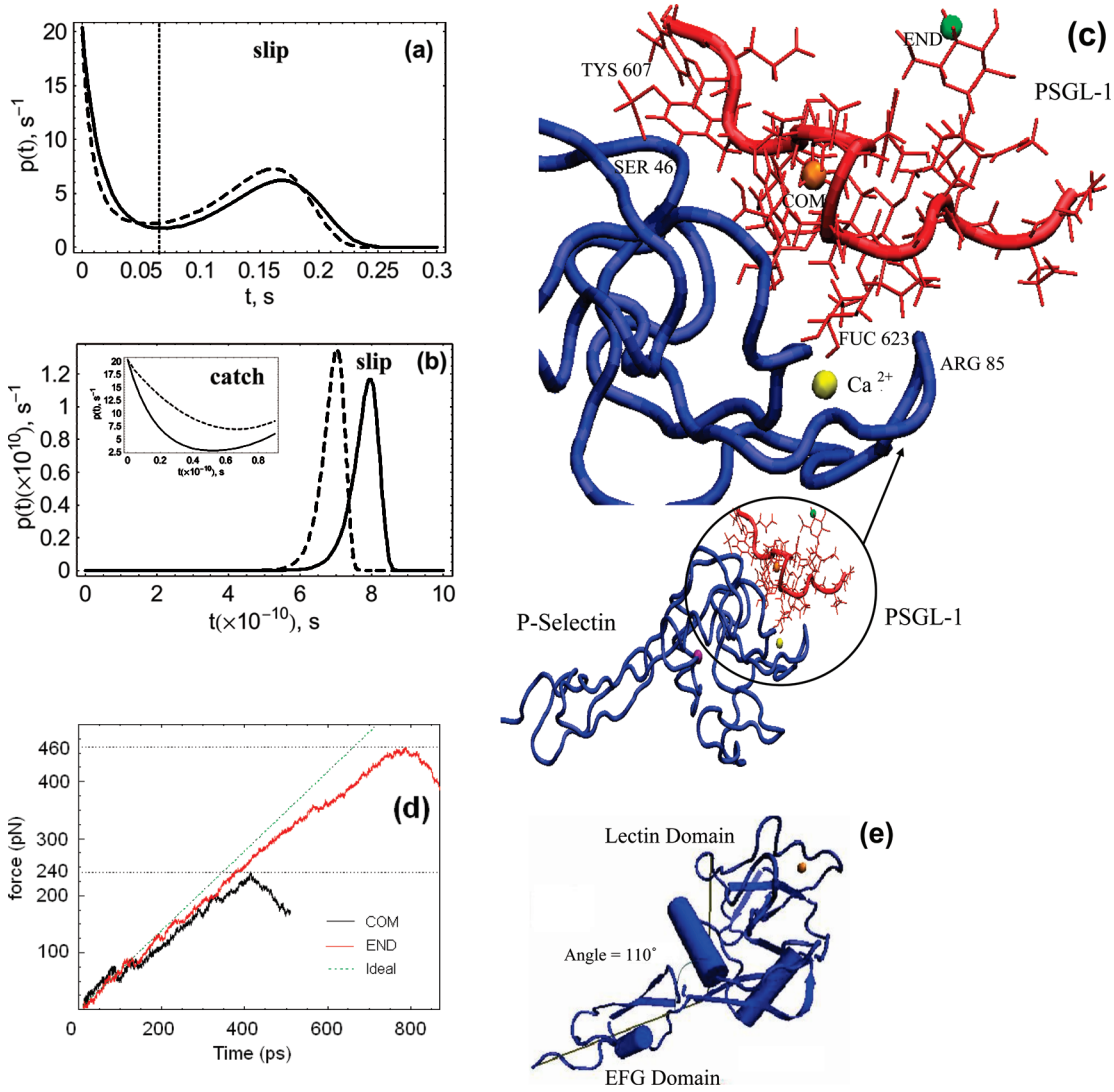

FIGURE 7. Insights from atomistic simulations. (a) Bond dissociation probability density vs time for experimental ramp rate, $r = 500$ pN/s indicates good agreement between two-pathway[15] (solid line) and deformation[16] (dashes) models. Bond dissociates in catch and slip regimes with 40% and 60% probabilities, respectively. (b) Same as part a, but for simulation ramp rate $r = 0.695 \times 10^{12}$ pN/s. Bond dissociates predominantly in slip regime. (c) P-selectin/PSGL-1 structure. Bond is stretched by fixing receptor's center of mass (COM) and pulling ligand at either its COM or END, purple, orange, and green balls, respectively. Two distinct interaction regions involve attraction of Tys-607 (Tys = sulfotyrosine) to Ser-46, and Fuc-623 (Fuc = fucose) to Ca^{2+} and nearby Arg-85. (d) Force dynamics in COM and END simulations. Force acting on the bond (solid line) differs from ideal ramp force (dashes) due to bond extension. (e) Angle between lectin and EFG domains opens from 110° to 125° after 800 ps of END simulation, supporting sliding–rebinding[24] and allosteric deformation models,[33] Figure 2d,e.

such as selectin/PSGL-1, where surface binding dominates, Figure 7c. Simulations indicate that the conceptually more involved deformation[16] and allosteric deformation[48] models may provide more realistic mechanisms of catch binding.

Conclusions and Outlook

The catch binding examples discussed above are but a few unique illustrations of the complexity and richness in biology. This Account reviewed the fundamental physical concepts proposed to explain catch binding, elaborated on the role of protein–water interaction, characterized typical measurement protocols, and evaluated utility of atomistic simulation.

Catch binding and its transformation to typical slip binding relies on a variety of responses of biological bonds to force. The catch–slip transition can occur if the bond switches between two dissociation pathways with growing force. Alternatively, force-induced conformational changes in receptor or ligand can improve the interaction. In addition to multiple dissociation pathways or protein conforma-

tional flexibility, further conditions are required for catch binding. The simplicity of the two-pathway and deformation models that use a minimal number of parameters leads to analytic expressions for the catch-binding conditions and bond lifetimes. Universal laws relate different measurement regimes and represent experimental data in concise and efficient ways.

The concepts developed for catch binding are general and clarify unusual observations seen with other biological bonds. The bond deformation concept rationalizes discrepancies between bond lifetimes seen with and without force. It characterizes biological bonds as stiff or deformable, and indicates whether receptor−ligand interaction is already optimized or can be improved by conformational changes. Recent experiments and simulations suggest that catch binding is associated with allosteric deformations, in which force-induced rearrangements far away from the binding site alter the site properties.

Protein−water interaction adds further twist to the catch-bond story by creating another form of catch binding at low forces. Moreover, the interaction explains the significant drop in stability of many bonds subjected to small perturbations, suggesting that biological systems can be efficiently activated by weak mechanical contacts, concentration gradients, or electric signals.

Molecular dynamics simulations generate valuable insights into catch binding and provide atomistic description of bond dissociation and conformational changes that precede and follow the main event. Despite the well-known time and length scale limitations of atomistic simulation, it remains an indispensable visualization tool, justifying analytic models and differentiating alternative interpretations of experiments.

Analogs of catch binding can be found in other biological and chemical systems. For instance, the time of peptide translocation through nanopores is maximized by electric field, as described with essentially the same two-pathway model.[15] The rate of disulfide bond reduction catalyzed by an enzyme can be enhanced by an applied force. The data were represented by a two-pathway model modified for concentration effects.[49] DNA double helix unwinds when pulled from opposite ends. However, at small forces DNA winds up tighter,[44] reminiscent of catch binding. Most materials expand upon heating, but some contract, creating negative thermal expansion.[50]

Only recently have scientists started to probe single molecules and molecular aggregates using carefully controlled forces. The omnipresence of chemical, mechanical, and electrical forces in living organisms suggests that more fascinating and counterintuitive phenomena akin to catch binding shall be discovered in the future. The ideas and concepts described in this Account provide the basic theoretical framework for such studies.

We are grateful to Evgeni Sokurenko and Wendy Thomas for illuminating discussions. Financial support of National Science Foundation, National Institute of Health, Department of Energy, and ACS Petroleum Research Fund is gratefully acknowledged.

BIOGRAPHICAL INFORMATION

Oleg Prezhdo obtained Diploma in Theoretical Chemistry in 1991 from Kharkov National University, Ukraine, working on many-body electronic structure theory and electron-vibrational dynamics under Anatoly Luzanov. From 1991 to 1993, he developed a continuum model of molecular solvation with Stanislav Tyurin in Kharkov Polytechnic University. Having moved to the U.S.A. in the fall of 1993, he completed his Ph.D. on nonadiabatic chemical dynamics under Peter Rossky at UT-Austin in 1997. After a brief postdoctoral fellowship with John Tully at Yale, where he worked on constrained density-functional theory, he moved to University of Washington in Seattle in 1998. In 2002, he was promoted to Associate Professor and in 2005 to Full Professor. In 2008, he became Senior Editor of the *Journal of Physical Chemistry* and was elected Fellow of the American Physical Society. His research interests range from fundamental aspects of semiclassical dynamics to photoexcitations in nanomaterials, to structural phase transitions, and to biological catch bonds.

Yuriy Pereverzev received his Ph.D. in theoretical physics from Rostov State University, Russia, in 1972 for investigation of transfer phenomena in ferro- and antiferromagnetics subjected to magnetic fields at low temperatures. From 1970 to 1999, he was Junior Research Fellow, Senior Research Fellow, and Leading Research Fellow in the Institute for Low Temperature Physics and Engineering in Kharkov, Ukraine. He investigated ground states, energy spectra, kinetic properties, phase diagrams, and absorption spectra of low-dimensional magnetic materials. He obtained the degree of Doctor of Science in 1990. In 1991, he received the State Science Award of the Ukraine. Since 1999, he has been Senior Research Scientist at the University of Washington in Seattle. Currently, his research focuses on nonlinear quantum dynamics, phase transitions of dipolar chromophores, and proteins subjected to mechanical forces.

FOOTNOTES

* Corresponding author. E-mail: prezhdo@u.washington.edu.

REFERENCES

1 Dembo, M.; Torney, D. C.; Saxman, K.; Hammer, D. The reaction-limited kinetics of membrane-to-surface adhesion and detachment. *Proc. R. Soc. London, Ser. B* **1988**, *234* (1274), 55–83.

2 Bell, G. I. Models for specific adhesion of cells to cells. *Science* **1978**, *200* (4342), 618–627.

3 Thomas, W. E.; Trintchina, E.; Forero, M.; Vogel, V.; Sokurenko, E. V. Bacterial adhesion to target cells enhanced by shear force. *Cell* **2002**, *109* (7), 913–923.

4 Isberg, R. R.; Barnes, P. Dancing with the host: Flow-dependent bacterial adhesion. *Cell* **2002**, *110* (1), 1–4.

5 Marshall, B. T.; Long, M.; Piper, J. W.; Yago, T.; McEver, R. P.; Zhu, C. Direct observation of catch bonds involving cell-adhesion molecules. *Nature* **2003**, *423* (6936), 190–193.

6 Sarangapani, K. K.; Yago, T.; Klopocki, A. G.; Lawrence, M. B.; Fieger, C. B.; Rosen, S. D.; McEver, R. P.; Zhu, C. Low force decelerates L-selectin dissociation from P-selectin glycoprotein ligand-1 and endoglycan. *J. Biol. Chem.* **2004**, *279* (3), 2291–2298.

7 Forero, M.; Thomas, W. E.; Bland, C.; Nilsson, L. M.; Sokurenko, E. V.; Vogel, V. A catch-bond based nanoadhesive sensitive to shear stress. *Nano Lett.* **2004**, *4* (9), 1593–1597.

8 Guo, B.; Guilford, W. H. Mechanics of actomyosin bonds in different nucleotide states are tuned to muscle contraction. *Proc. Natl. Acad. Sci. U.S.A.* **2006**, *103* (26), 9844–9849.

9 McEver, R. P. Selectins: Lectins that initiate cell adhesion under flow. *Curr. Opin. Cell. Biol.* **2002**, *14*, 581–586.

10 Zhu, C.; Yago, T.; Lou, J. Z.; Zarnitsyna, V. I.; McEver, R. P. Mechanisms for flow-enhanced cell adhesion. *Ann. Biomed. Eng.* **2008**, *36* (4), 604–621.

11 Zhu, C.; Lou, J. Z.; McEver, R. P. Catch bonds: Physical models, structural bases, biological function and rheological relevance. *Biorheology* **2005**, *42* (6), 443–462.

12 Bartolo, D.; Derenyi, I.; Ajdari, A. Dynamic response of adhesion complexes: Beyond the single-path picture. *Phys. Rev. E* **2002**, *65* (5), 051910.

13 Evans, E.; Leung, A.; Heinrich, V.; Zhu, C. Mechanical switching and coupling between two dissociation pathways in a P-selectin adhesion bond. *Proc. Natl. Acad. Sci. U.S.A.* **2004**, *101* (31), 11281–11286.

14 Barsegov, V.; Thirumalai, D. Dynamics of unbinding of cell adhesion molecules: Transition from catch to slip bonds. *Proc. Natl. Acad. Sci. U.S.A.* **2005**, *102* (6), 1835–1839.

15 Pereverzev, Y. V.; Prezhdo, O. V.; Forero, M.; Sokurenko, E. V.; Thomas, W. E. The two-pathway model for the catch-slip transition in biological adhesion. *Biophys. J.* **2005**, *89* (3), 1446–1454.

16 Pereverzev, Y. V.; Prezhdo, O. V. Force-induced deformations and stability of biological bonds. *Phys. Rev. E* **2006**, *73*, 050902.

17 Thomas, W.; Forero, M.; Yakovenko, O.; Nilsson, L.; Vicini, P.; Sokurenko, E.; Vogel, V. Catch-bond model derived from allostery explains force-activated bacterial adhesion. *Biophys. J.* **2006**, *90* (3), 753–764.

18 Aprikian, P.; Tchesnokova, V.; Kidd, B.; Yakovenko, O.; Yarov-Yarovoy, V.; Trinchina, E.; Vogel, V.; Thomas, W.; Sokurenko, E. Interdomain interaction in the FimH adhesin of *Escherichia coli* regulates the affinity to mannose. *J. Biol. Chem.* **2007**, *282* (32), 23437–23446.

19 Nilsson, L. M.; Thomas, W. E.; Sokurenko, E. V.; Vogel, V. Beyond induced-fit receptor-ligand interactions: Structural changes that can significantly extend bond lifetimes. *Structure* **2008**, *16* (7), 1047–1058.

20 Lou, J. Z.; Yago, T.; Klopocki, A. G.; Mehta, P.; Chen, W.; Zarnitsyna, V. I.; Bovin, N. V.; Zhu, C.; McEver, R. P. Flow-enhanced adhesion regulated by a selectin interdomain hinge. *J. Cell Biol.* **2006**, *174* (7), 1107–1117.

21 Lou, J. Z.; Zhu, C. Sliding-rebinding mechanism governs glycoprotein Ib/von Willebrand factor catch bonds. *Blood* **2007**, *110* (11), 1086A–1087A.

22 Liu, F.; Ou-Yang, Z. C.; Iwamoto, M. Dynamic disorder in receptor−ligand forced dissociation experiments. *Phys. Rev. E* **2006**, *73* (1), 010901.

23 Marshall, B. T.; Sarangapani, K. K.; Lou, J. H.; McEver, R. P.; Zhu, C. Force history dependence of receptor-ligand dissociation. *Biophys. J.* **2005**, *88* (2), 1458–1466.

24 Lou, J. Z.; Zhu, C. A structure-based sliding-rebinding mechanism for catch bonds. *Biophys. J.* **2007**, *92* (5), 1471–1485.

25 Yago, T.; Lou, J.; Wu, J.; Yang, j.; Miner, J. J.; Coburn, L.; López, J. A.; Cruz, M. A.; Dong, J.-F.; McIntire, L. V.; McEver, R. P.; Zhu, C. Platelet glycoprotein Ibα forms catch bonds with human WT vWF but not with type 2B von Willebrand disease vWF. *J. Clin. Invest.* **2008**, *118* (9), 3195–3207.

26 Pereverzev, Y. V.; Prezhdo, O. V.; Thomas, W. E.; Sokurenko, E. V. Distinctive features of the biological catch bond in the jump-ramp force regime predicted by the two-pathway model. *Phys. Rev. E* **2005**, *72* (1), 010903.

27 Pereverzev, Y. V.; Prezhdo, O. V. Universal laws in the force-induced unraveling of biological bonds. *Phys. Rev. E* **2007**, *75*, 011905.

28 Pereverzev, Y. V.; Prezhdo, O. V. Dissociation of biological catch-bond by periodic perturbation. *Biophys. J.* **2006**, *91* (2), L19–L21.

29 Jadhav, S.; Eggleton, C. D.; Konstantopoulos, K. A 3-D computational model predicts that cell deformation affects selectin-mediated leukocyte rolling. *Biophys. J.* **2005**, *88* (1), 96–104.

30 Yakovenko, O.; Sharma, S.; Forero, M.; Tchesnokova, V.; Aprikian, P.; Kidd, B.; Mach, A.; Vogel, V.; Sokurenko, E.; Thomas, W. E. FimH forms catch bonds that are enhanced by mechanical force due to allosteric regulation. *J. Biol. Chem.* **2008**, *283* (17), 11596–11605.

31 Tchesnokova, V.; Aprikian, P.; Yakovenko, O.; Larock, C.; Kidd, B.; Vogel, V.; Thomas, W.; Sokurenko, E. Integrin-like allosteric properties of the catch bond-forming FimH adhesin of *Escherichia coli*. *J. Biol. Chem.* **2008**, *283* (12), 7823–7833.

32 Ronald, L. S.; Yakovenko, O.; Yazvenko, N.; Chattopadhyay, S.; Aprikian, P.; Thomas, W. E.; Sokurenko, E. V. Adaptive mutations in the signal peptide of the type 1 fimbrial adhesin of uropathogenic *Escherichia coli*. *Proc. Natl. Acad. Sci. U.S.A.* **2008**, *105* (31), 10937–10942.

33 Gunnerson, K. N.; Pereverzev, Y. V.; Prezhdo, O. V. Atomistic simulations combined with analytic theory to study the response of the P-selectin/PSGL-1 complex to an external force. *J. Phys. Chem. B* **2009**, *113*, 2090–2100.

34 Cui, Q.; Karplus, M. Allostery and cooperativity revisited. *Protein Sci.* **2008**, *17* (8), 1295–307.

35 Xiao, T.; Takagi, J.; Coller, B. S.; Wang, J. H.; Springer, T. A. Structural basis for allostery in integrins and binding to fibrinogen-mimetic therapeutics. *Nature* **2004**, *432* (7013), 59–67.

36 Thomas, W. E.; Vogel, V.; Sokurenko, E. Biophysics of catch bonds. *Annu. Rev. Biophys.* **2008**, *37*, 399–416.

37 Thomas, W. Catch bonds in adhesion. *Annu. Rev. Biomed. Eng.* **2008**, *10*, 39–57.

38 Phan, U. T.; Waldron, T.; Springer, T. A. Remodeling of the lectin-EGF-like domain interface in P- and L-selectin increases adhesiveness and shear resistance under hydrodynamic force. *Nat. Immunol.* **2006**, *7* (8), 883–889.

39 Merkel, R.; Nassoy, P.; Leung, A.; Ritchie, K.; Evans, E. Energy landscapes of receptor-ligand bonds explored with dynamic force spectroscopy. *Nature* **1999**, *397* (6714), 50–53.

40 Jung, L. S.; Nelson, K. E.; Stayton, P. S.; Campbell, C. T. Binding and dissociation kinetics of wild-type and mutant streptavidins on mixed biotin-containing alkylthiolate monolayers. *Langmuir* **2000**, *16* (24), 9421–9432.

41 Pereverzev, Y. V.; Prezhdo, O. V.; Sokurenko, E. V. Anomalously increased lifetimes of biological complexes at zero force due to the protein−water Interface. *J. Phys. Chem. B* **2008**, *112*, 11440–11445.

42 Fritz, J.; Katopodis, A. G.; Kolbinger, F.; Anselmetti, D. Force-mediated kinetics of single P-selectin ligand complexes observed by atomic force microscopy. *Proc. Natl. Acad. Sci. U.S.A.* **1998**, *95* (21), 12283–12288.

43 Hornblower, B.; Coombs, A.; Whitaker, R. D.; Kolomeisky, A.; Picone, S. J.; Meller, A.; Akeson, M. Single-molecule analysis of DNA-protein complexes using nanopores. *Nat. Methods* **2007**, *4* (4), 315–317.

44 Gore, J.; Bryant, Z.; Nollmann, M.; Le, M. U.; Cozzarelli, N. R.; Bustamante, C. DNA overwinds when stretched. *Nature* **2006**, *442* (7104), 836–839.

45 Fisher, M. E.; Kolomeisky, A. B. Simple mechanochemistry describes the dynamics of kinesin molecules. *Proc. Natl. Acad. Sci. U.S.A.* **2001**, *98* (14), 7748–7753.

46 Phillips, J. C.; Braun, R.; Wang, W.; Gumbart, J.; Tajkhorshid, E.; Villa, E.; Chipot, C.; Skeel, R. D.; Kale, L.; Schulten, K. Scalable molecular dynamics with NAMD. *J. Comput. Chem.* **2005**, *26* (16), 1781–1802.

47 Somers, W. S.; Tang, J.; Shaw, G. D.; Camphausen, R. T. Insights into the molecular basis of leukocyte tethering and rolling revealed by structures of P- and E-selectin bound to SLe(X) and PSGL-1. *Cell* **2000**, *103* (3), 467–479.

48 Pereverzev, Y. V.; Prezhdo, O. V.; Sokurenko, E. V., Allosteric deformation model of the biological catch bond. *Phys. Rev. E* **2008**,submitted for publication.

49 Wiita, A. P.; Perez-Jimenez, R.; Walther, K. A.; Grater, F.; Berne, B. J.; Holmgren, A.; Sanchez-Ruiz, J. M.; Fernandez, J. M. Probing the chemistry of thioredoxin catalysis with force. *Nature* **2007**, *450* (7166), 124–127.

50 Mary, T. A.; Evans, J. S. O.; Vogt, T.; Sleight, A. W. Negative thermal expansion from 0.3 to 1050 Kelvin in ZrW_2O_8. *Science* **1996**, *272* (5258), 90–92.